PSFC/JA-06-25

Plasma shaping effects on the collisionless residual zonal flow level

Yong Xiao and Peter J. Catto

MIT Plasma Science and Fusion Center,
167 Albany Street,
Cambridge, MA 02139, U.S.A.

This work was supported by the U.S. Department of Energy, Grant No. DE-FG02-91ER-54109.

Submitted for publication in the Physics of Plasma

Plasma shaping effects on the collisionless residual zonal flow level

Yong Xiao and and Peter J. Catto

MIT Plasma Science and Fusion Center, Cambridge, MA 02139, U.S.A.

(Dated: 6/15/2006)

Abstract

Plasma shaping effects, such as elongation, triangularity and *Shafranov* shift have long been considered an important ingredient in improving tokamak performance. It is known that the growth rate of ion temperature gradient (ITG) turbulence can be regulated by these shaping effects and that the ITG turbulence level can also be regulated by zonal flow. Moreover, recent numerical simulation shows that the collsionless residual zonal flow level can be influenced by these shaping effects. An analytical approach is used to explicitly evaluate plasma shaping effects on the collisionless residual zonal flow. The results show that the residual zonal flow level increases with elongation, triangularity and the *Shafranov* shift.

I. INTRODUCTION

Rosenbluth and *Hinton* [1] evaluated the collisionless residual zonal flow level for a large aspect ratio circular flux surface tokamak cross section. Their procedure [1][2] can be generalized to retain the effects of elongation, the *Shafranov* shift and triangularity by using a model equilibrium [3][4]. Shaping is known to have a strong effect on the tokamak confinement [5]. In particular, numerical studies show that the growth rate of ion temperature gradient (ITG) turbulence can have a strong dependence on these shaping effects [6]. Moreover, it is known that zonal flow is an important tool in regulating ITG turbulence [7][8][9]. A recent study using the gyrokinetic code *GS2* to examine zonal flow [10] finds that the collisionless residual zonal flow level is strongly influenced by the plasma shape. However, an ab initio analytical treatment is still desirable. Here we consider an analytical approach based on an inverse aspect ratio expansion. The calculation employs a local MHD equilibrium that contains the elongation and triangularity of the plasma shape, as well as the dependence on safety factor and the *Shafranov* shift. The result shows that the residual zonal flow level increases strongly with elongation, and moderately with the *Shafranov* shift and triangularity.

In the *Rosenbluth-Hinton* (*R-H*) zonal flow model, [1][2] the initial zonal flow potential is shielded by classical polarization due to gyromotion departure from a flux surface. After several bounce periods, the zonal flow potential is shielded by the total plasma polarization that also contains the drift departure from a flux surface. In the large radial wavelength limit, the total plasma polarization contains both classical polarization and neoclassical polarization. The residual zonal flow level is then given by [2]

$$\phi_k(\infty) = \frac{\phi_k(0)}{1 + \frac{m_i (IS')^2}{n_0 T_i \left\langle k_\perp^2 / B^2 \right\rangle} \left\langle \int d^3v F_0 \frac{v_\parallel}{B} \left[\frac{v_\parallel}{B} - \overline{\left(\frac{v_\parallel}{B}\right)} \right] \right\rangle}, \tag{1}$$

where F_0 is a local *Maxwellian*, $\mathbf{k}_\perp = \nabla S$ is the perpendicular wave vector, $S = S(\psi)$ is the eikonal of perturbed quantities, $\langle A \rangle \equiv \oint \frac{dl_p}{B_p} A / \oint \frac{dl_p}{B_p}$ is the flux surface average, and $\overline{A} \equiv \oint \frac{dl}{v_\shortparallel} A / \oint \frac{dl}{v_\shortparallel}$ is the bounce average of quantity A. The original *R-H* treatment utilizes a large aspect ratio circular tokamak model [1] and shows that the residual zonal flow level is given by

$$\phi_k(\infty) = \frac{\phi_k(0)}{1 + 1.6 q^2 / \sqrt{\varepsilon}}, \tag{2}$$

where the factor of unity is classical and the $q^2/\sqrt{\varepsilon}$ neoclassical. This calculation can be extended to include the important plasma shaping effects, such as elongation, *Shafranov* shift and triangularity. To do so we discuss the MHD equilibrium employed in Sec. II. This equilibrium is a simple limit [3][4] of the *Miller* equilibrium [11] in which the radial variations of elongation, triangularity, safety factor and pressure are ignored. In Sec. III we present the detailed evaluation of the effects of shaping. A brief discussion of our results follows in Sec. IV.

II. GLOBAL MHD EQUILIBRIUM

It is difficult to find an analytically tractable MHD equilibrium which contains all the important plasma cross section ingredients. However, for constant $dp/d\psi$ and $IdI/d\psi$, there exists an MHD equilibrium that satisfies the *Grad-Shafranov* equation, where p is the total pressure and $I = RB_T$ with R the major radius and B_T the toroidal magnetic field [3][4]. In this limit, the poloidal flux function is written in the form

$$\psi(R,Z) = \frac{\psi_0}{R_0^4}[\left(R^2 - R_0^2\right)^2 + \frac{Z^2}{E^2}\left(R^2 - R_x^2\right) - \tau R_0^2(R^2 \ln\frac{R^2}{R_0^2} - \left(R^2 - R_0^2\right) - \frac{\left(R^2 - R_0^2\right)^2}{2R_0^2})], \tag{3}$$

where the constant ψ_0 sets the magnitude of the poloidal magnetic flux ψ, the constant R_0 represents the radial location of magnetic axis where $\psi = 0$, and R_x is the radial X point location. The constants E, τ and R_x in the preceding equation are functions of the *Shafranov* shift (Δ), elongation (κ) and triangularity (δ). In spite of the assumption of constant $dp/d\psi$ and $IdI/d\psi$, this global equilibrium is a good approximation for many cases of interest.

Near the magnetic axis the magnetic flux becomes an approximate ellipse satisfying

$$\frac{\psi(x,z)}{\psi_0} = 4(x+s)^2 + \frac{z^2}{E^2}\left(1 - \frac{R_x^2}{R_0^2}\right), \tag{4}$$

where the shift s is defined as

$$s = \left(1 + \frac{\tau}{3}\right)\frac{x^2}{2} + \frac{z^2}{4E^2}, \tag{5}$$

and the dimensionless variables x and z are defined by

$$R = R_0(1+x), \tag{6}$$

$$Z = R_0 z. \tag{7}$$

We change variables from (x, z) to (ε, θ) by letting

$$x = \varepsilon \cos\theta - \Delta \cos^2\theta - \frac{\kappa^2}{4E^2}\varepsilon^2 \sin^2\theta, \tag{8}$$

$$z = \kappa\varepsilon \sin\theta. \tag{9}$$

where ε is the inverse aspect ratio, θ is the poloidal angle, the flux function

$$\Delta = \left(1 + \frac{\tau}{3}\right)\frac{\varepsilon^2}{2} \tag{10}$$

is the dimensionless *Shafranov* shift, and the constant κ is the elongation of the flux shape defined by

$$\kappa \equiv \frac{2E}{\sqrt{1 - R_x^2/R_0^2}}. \tag{11}$$

The triangularity δ associated with Eqs. (8) and (9) is defined by $\delta \equiv (x_c - x_m)/\varepsilon$, where $x_m = -(\varepsilon\kappa/2E)^2$ is the major radius at which z reaches the highest point on the flux surface, and $x_c = -\Delta$ is the major radius at the center of flux surface. Using Eqs. (8) and (9) we find

$$\delta = \left[\frac{\kappa^2}{4E^2} - \frac{\Delta}{\varepsilon^2}\right]\varepsilon = \frac{\varepsilon}{1 - R_x^2/R_0^2} - \frac{\Delta}{\varepsilon}, \tag{12}$$

where to the requisite order, the flux function becomes

$$\psi = 4\psi_0\varepsilon^2, \tag{13}$$

making the inverse aspect ratio ε a flux label. To simplify the notation, we introduce the following two order unity constants

$$\widetilde{A} \equiv \frac{\Delta}{\varepsilon^2}, \tag{14}$$

$$\widetilde{B} \equiv \frac{\Delta}{\varepsilon^2} + \frac{\delta}{\varepsilon}. \tag{15}$$

Then, the magnetic flux can be written in the following way:

$$R = R_0\left(1 + \varepsilon\cos\theta - \widetilde{A}\varepsilon^2\cos^2\theta - \widetilde{B}\varepsilon^2\sin^2\theta\right),$$

$$Z = R_0\kappa\varepsilon\sin\theta. \tag{16}$$

Some quantities, such as the magnetic field B and the volume element dl_p/B_p, are required to evaluate the polarization in Eq. (1). The preceding local equilibrium provides a simple

inverse aspect ratio expansion for these quantities. The poloidal magnetic field is computed from $B_p = |\nabla\psi|/R = 8\psi_0\varepsilon\,|\nabla\varepsilon|/R$, giving

$$B_p = \frac{8\psi_0\varepsilon}{\kappa R_0^2}\frac{\eta}{\left(1-2\widetilde{A}\varepsilon\cos\theta\right)\left(1+\varepsilon\cos\theta-\widetilde{A}\varepsilon^2\cos^2\theta-\widetilde{B}\varepsilon^2\sin^2\theta\right)}, \tag{17}$$

where the numerator η is defined as

$$\eta = \sqrt{\kappa^2\cos^2\theta+\sin^2\theta+4\varepsilon\sin^2\theta\cos\theta\left(\widetilde{B}-\widetilde{A}\right)+4\varepsilon^2\sin^2\theta\cos^2\theta\left(\widetilde{B}-\widetilde{A}\right)^2}. \tag{18}$$

The safety factor q depends on the poloidal field and is defined by

$$q(\psi) \equiv \frac{I(\psi)}{2\pi}\oint\frac{dl_p}{R^2B_p}, \tag{19}$$

where the poloidal arc length $dl_p = \eta R_0\varepsilon d\theta$ and $I = RB_T$ with B_T the toroidal field. For a large aspect ratio tokamak, Eq. (19) may be first expanded in ε and then integrated over θ to obtain

$$q = \frac{\kappa R_0 I}{8\psi_0}\left[1+\frac{1}{2}\left(1+3\widetilde{A}+\widetilde{B}\right)\varepsilon^2+\mathcal{O}\left(\varepsilon^4\right)\right]. \tag{20}$$

Then, the poloidal field B_p can be expressed in terms of this safety factor

$$B_p = \frac{I}{R_0}\frac{\varepsilon}{q}\sqrt{\kappa^2\cos^2\theta+\sin^2\theta}\,(1+\mathcal{O}(\varepsilon)). \tag{21}$$

The volume element dl_p/B_p can also be expanded in ε to obtain

$$\begin{aligned}\frac{dl_p}{B_p} = {}& \frac{q}{I}R_0^2 d\theta\left(1-2\widetilde{A}\varepsilon\cos\theta\right)\left(1+\varepsilon\cos\theta-\widetilde{A}\varepsilon^2\cos^2\theta-\widetilde{B}\varepsilon^2\sin^2\theta\right)\\ &\left[1-\frac{1}{2}\left(1+3\widetilde{A}+\widetilde{B}\right)\varepsilon^2+\mathcal{O}\left(\varepsilon^4\right)\right].\end{aligned} \tag{22}$$

In addition, to $\mathcal{O}(\varepsilon^2)$, the magnetic field B and its inverse $1/B$ can be expanded in ε to find

$$B = B_0\left\{1-\varepsilon\cos\theta+\varepsilon^2\left[\left(\widetilde{A}+1+\frac{\kappa^2}{2q^2}\right)\cos^2\theta+\left(\widetilde{B}+\frac{1}{2q^2}\right)\sin^2\theta\right]\right\}, \tag{23}$$

$$\frac{1}{B} = \frac{1}{B_0}\left\{1+\varepsilon\cos\theta-\varepsilon^2\left[\left(\widetilde{A}+\frac{\kappa^2}{2q^2}\right)\cos^2\theta+\left(\widetilde{B}+\frac{1}{2q^2}\right)\sin^2\theta\right]\right\}, \tag{24}$$

where B_0 is defined by $B_0 \equiv I/R_0 = RB_T/R_0$. In this local equilibrium model, the trapped-passing boundary is given by

$$\lambda_c = 1-\varepsilon-\varepsilon^2\left(\widetilde{A}+\frac{\kappa^2}{2q^2}\right). \tag{25}$$

III. COLLISIONLESS RESIDUAL ZONAL FLOW LEVEL

Using the local equilibrium model from the preceding section, the collisionless residual zonal flow level in Eq. (1) can be evaluated. The perpendicular wave vector $k_\perp = S' \left|\nabla\psi\right|$ gives

$$\left\langle \frac{k_\perp^2}{B^2} \right\rangle = \left(IS' \frac{\varepsilon}{q} \right)^2 \left[1 + \left(1 + 3\widetilde{A} + \widetilde{B} \right) \varepsilon^2 \right] \frac{\oint \frac{dl_p}{B_p} \frac{\eta^2}{B^2 \left(1 - 2\widetilde{A}\varepsilon\cos\theta \right)^2}}{\oint \frac{dl_p}{B_p}}. \tag{26}$$

A small ε expansion can be employed to evaluate the preceding equation. Since the volume element dl_p/B_p appears in both the numerator and denominator, it can be replaced in such ratios by

$$\frac{dl_p}{B_p} \rightarrow d\theta \left(1 - 2\widetilde{A}\varepsilon\cos\theta \right) \left(1 + \varepsilon\cos\theta - \widetilde{A}\varepsilon^2\cos^2\theta - \widetilde{B}\varepsilon^2\sin^2\theta \right) \tag{27}$$

without changing the solution. Therefore,

$$\left\langle \frac{k_\perp^2}{B^2} \right\rangle = \left(IS' \frac{\varepsilon}{q} \right)^2 \frac{\pi \left(1 + \kappa^2 \right)}{\oint \frac{dl_p}{B_p}} \left[1 + \mathcal{O}\left(\varepsilon^2 \right) \right], \tag{28}$$

with dl_p/B_p given by Eq. (27), and

$$\oint \frac{dl_p}{B_p} \rightarrow 2\pi \left[1 - \frac{\varepsilon^2}{2} \left(3\widetilde{A} + \widetilde{B} \right) \right], \tag{29}$$

where the use of an arrow indicates that Eq. (27) is employed.

The next step is to evaluate $\left\langle \int d^3v F_0 v_\parallel^2 / B^2 \right\rangle$ in Eq. (1) for this local equilibrium. Note first that $\left\langle \int d^3v F_0 v_\parallel^2 / B^2 \right\rangle = \left\langle 1/B^2 \right\rangle n_0 T_i / m_i$. Then, using Eq. (24) and applying the small ε expansion, it is easy to obtain

$$\left\langle \int d^3v F_0 \frac{v_\parallel^2}{B^2} \right\rangle = \frac{n_0 T_i}{m_i B_0^2} \frac{2\pi}{\oint \frac{dl_p}{B_p}} \left\{ 1 - \left[\frac{3}{2} (3\widetilde{A} + \widetilde{B} - 1) + \frac{1 + \kappa^2}{2q^2} \right] \varepsilon^2 \right\}, \tag{30}$$

where $\oint dl_p/B_p$ is given by Eq. (29).

The evaluation of $\left\langle \int d^3v F_0 \overline{\left(v_\parallel / B \right)} v_\parallel / B \right\rangle$ in Eq. (1) is much more involved. Fortunately only the passing particle contribution needs to be considered, leading to

$$\left\langle \int d^3v F_0 \overline{\left(\frac{v_\parallel}{B} \right)^2} \right\rangle = \frac{3 n_0 T_i}{2 m_i B_0^2} \oint \frac{dl_p}{B_p} \int_0^{\lambda_c} d\lambda \frac{1}{\oint \frac{dl_p}{B_p} \frac{B}{B_0 \xi}}, \tag{31}$$

where the trapped-passing boundary λ_c is defined in Eq. (25), and $\xi = \left| v_\parallel \right| / v$. The integral $\oint \frac{dl_p}{B_p} \frac{B}{B_0 \xi}$ can be written as

$$\oint \frac{dl_p}{B_p} \frac{B}{B_0 \xi} = \oint \frac{dl_p}{B_p} \frac{\sqrt{B/B_0}}{\sqrt{B_0/B - \lambda}}, \tag{32}$$

where we already have expressions for B_0/B and B/B_0 in Eqs. (24) and (23). Using these expressions, we find

$$\frac{1}{\sqrt{B_0/B-\lambda}}=\frac{1}{\sqrt{1-\lambda+\varepsilon\cos\theta-\left[\left(\widetilde{A}+\frac{\kappa^2}{2q^2}\right)\cos^2\theta+\left(\widetilde{B}+\frac{1}{2q^2}\right)\sin^2\theta\right]\varepsilon^2}}. \tag{33}$$

Recalling Eq. (27), we have

$$\begin{aligned}\frac{dl_p}{B_p}\sqrt{B/B_0}\rightarrow d\theta\{1+\varepsilon\left(\frac{1}{2}-2\widetilde{A}\right)\cos\theta+[(-\frac{1}{8}+\frac{3}{2}\widetilde{A}\\ +\frac{\kappa^2}{4q^2})\cos^2\theta+(-\frac{1}{2}\widetilde{B}+\frac{1}{4q^2})\sin^2\theta]\varepsilon^2\}.\end{aligned} \tag{34}$$

We next let $\tau=1-\lambda$, with $\varepsilon<\tau\leq 1$ for the passing particles. Then, $1/\sqrt{B_0/B-\lambda}$ may be expanded in powers of ε to obtain

$$\begin{aligned}\frac{1}{\sqrt{B_0/B-\lambda}}=\frac{1}{\sqrt{\tau}}(1-\frac{1}{2}\frac{\varepsilon\cos\theta}{\tau}+\frac{1}{2}\frac{\varepsilon^2}{\tau}(\left(\widetilde{A}+\frac{\kappa^2}{2q^2}\right)\cos^2\theta+\\ \left(\widetilde{B}+\frac{1}{2q^2}\right)\sin^2\theta)+\frac{3}{8}\frac{\varepsilon^2}{\tau^2}\cos^2\theta+....+\mathcal{O}\left(\varepsilon^{M+1}\right),\end{aligned} \tag{35}$$

where the expansion order M depends on the desired accuracy of the final integral in Eq. (31). Therefore, the integrand of $\oint\frac{dl_p}{B_p}\frac{B}{B_0\xi}$ can be expressed as an ε expansion with the coefficients to be polynomials in $1/\tau$. As a result, Eq. (31) can be integrated to obtain the ε expansion [12]

$$\begin{aligned}\left\langle\int d^3v F_0\overline{\left(\frac{v_\parallel}{B}\right)}^2\right\rangle=\frac{n_0T_i}{m_iB_0^2}\frac{2\pi}{\oint\frac{dl_p}{B_p}}\{1-1.635\varepsilon^{3/2}-[\frac{1+\kappa^2}{2q^2}\\ +(\frac{3}{2}(3\widetilde{A}+\widetilde{B})-1)]\varepsilon^2-\frac{1}{2}(-0.722+1.502\widetilde{A}\\ +1.443\widetilde{B}+\frac{0.722-0.692\kappa^2}{q^2})\varepsilon^{5/2}\},\end{aligned} \tag{36}$$

that is accurate to $\mathcal{O}\left(\varepsilon^{5/2}\right)$. This equation together with Eq. (30) gives

$$\begin{aligned}&\left\langle\int d^3v F_0\overline{\left(\frac{v_\parallel}{B}\right)}^2\right\rangle-\left\langle\int d^3v F_0\overline{\left(\frac{v_\parallel^2}{B^2}\right)}\right\rangle\\ &=\frac{n_0T_i}{m_iB_0^2}\frac{2\pi}{\oint\frac{dl_p}{B_p}}[1.635\varepsilon^{3/2}+\frac{1}{2}\varepsilon^2-\frac{1}{2}(-0.722\\ &+1.502\widetilde{A}+1.443\widetilde{B}+\frac{0.722-0.692\kappa^2}{q^2})\varepsilon^{5/2}].\end{aligned} \tag{37}$$

The collisionless residual zonal flow level in Eq. (1) can be evaluated by using the preceding result and Eq. (28), to find

$$\phi_k(\infty) = \frac{\phi_k(0)}{1 + Sq^2/\sqrt{\varepsilon}}, \tag{38}$$

where the shaping function S is given by

$$S = \frac{1}{1+\kappa^2}(3.27 + \sqrt{\varepsilon} + 0.722\varepsilon - 1.443\delta \\ - 2.945\frac{\Delta}{\varepsilon} + \frac{0.692\kappa^2 - 0.722}{q^2}). \tag{39}$$

If $\kappa = 1$, $\delta = 0$, $\Delta = 0$, and $q \to \infty$, then the plasma shape becomes circular and the residual zonal flow level returns to the *R-H* value $\phi_k(0)/(1 + 1.6q^2/\sqrt{\varepsilon})$ but with higher order ε corrections retained that act to reduce the residual zonal flow level.

IV. CONCLUSION AND DISCUSSION

In the preceding section we obtained an analytical formula for the collisionless residual zonal flow level in a shaped plasma. This is the first analytical gyrokinetic treatment of zonal flow that incorporates the important plasma shaping effects associated with elongation, the *Shafranov* shift, and triangularity. It provides a benchmark for numerical codes to investigate shaping effects on zonal flow.

As shown in Figs. 1, 2 and 3, the residual zonal flow level increases with elongation, triangularity and *Shafranov* shift. From Eq. (39), we see that elongation is the leading order shaping effect, and that the *Shafranov* shift and triangularity are one order smaller in ε. Hence, the residual zonal flow level increases with elongation more rapidly than with the *Shafranov* shift and triangularity, as shown in the figures. This behavior is reasonable since in the equilibrium model, elongation is one order larger in ε than triangularity and the *Shafranov* shift. From Fig. 1, we see that when the elongation increases from 1 to 3, the residual zonal flow increases about 4 times. Recall that the energy associated with the zonal flow is $\propto |\phi_k|^2$. If we assume the increased zonal flow energy is due to energy transferred from the turbulence, then the turbulent transport may be reduced to one sixteenth by increasing the elongation from circular to 3. Therefore, this simple model shows the influence of elongation on turbulence is substantial.

A recent numerical study [10] yields a fit for elongation and triangularity with a dependence very similar to our analytical result. But for large elongation, this numerical calculation shows a stronger dependence on triangularity than our analytical model. However, the equilibrium model [11] in this numerical calculation includes not only the shaping parameters like elongation, triangularity, safety factor, and *Shafranov* shift, but also the radial gradients of them, and also takes the triangularity to be a function of elongation. This result may suggest that the gradients of these shaping parameters play a positive role in increasing the residual zonal flow. Although, it should be kept in mind that this *Miller* equilibrium as used in the code is a local solution to the *Grad-Shafranov* equation rather than a global solution as considered here. As a result, this local fit in the vicinity of a flux surface will fail for significant departures from the flux surface or if parameters are varied in a manner incompatible with it remaining a solution of the *Grad-Shafranov* equation. A comprehensive analytical model including the additional gradient effects that is also a global solution of the *Grad-Shafranov* equation might be possible for pressure and I^2 profiles linear in ψ; however, the expression for the residual may then be too complex to be useful.

ACKNOWLEDGEMENT

The authors are grateful to Dr. Jesus Ramos for helpful and enlightening discussions on the *Grad-Shafranov* equation.

This work was supported by U.S. Department of Energy Grant No. DE-FG02-91ER-54109 at the Massachusetts Institute of Technology.

REFERENCES

[1] M. Rosenbluth and F. Hinton, Phys. Rev. Lett. **80**, 724 (1998).

[2] F. Hinton and M. Rosenbluth, Plasma Phys. Control. Fusion **41**, A653 (1999).

[3] P. Helander and D. Sigmar, *Neoclassical Transport Theory*, Wiley, New York, 2001.

[4] S. Zheng, A. Wootton, and E. Solano, Phys. plasmas **3**, 1176 (1996).

[5] L. Lao and et al., Phys. Rev. Lett. **70**, 3435 (1993).

[6] R. Waltz and R. Miller, Phys. Plasmas **6**, 4265 (1999).

[7] W. Dorland and G. Hammett, Phys. Fluids B **5**, 812 (1993).

[8] Z. Lin, T. Hahm, W. Lee, W. Tang, and P. H. Diamond, Phys. Rev. Lett. **83**, 3645 (1999).

[9] J. Candy and R. Waltz, Phys. Rev. Lett. **91**, 045001 (2003).

[10] E. Belli, Ph.D. dissertation, Princeton University (2006).

[11] R. Miller, M. Chu, J. Greene, Y. Lin-Liu, and R. Waltz, Phys. Plasmas **5**, 973 (1998).

[12] Y. Xiao, Ph.D. dissertation, Massachusetts Institute of Technology (2006).

FIGURE CAPTIONS

Fig. 1 The residual zonal flow level varies with elongation κ for $q = 2$, $\varepsilon = 0.2$, $\Delta = 0.04$, and $\delta = 0$.

Fig. 2 The residual zonal flow level varies with triangularity δ for $q = 2$, $\varepsilon = 0.2$, $\Delta = 0.04$, and $\kappa = 1.8$.

Fig. 3 The residual zonal flow level varies with *Shafranov* shift Δ for $q = 2$, $\varepsilon = 0.2$, $\kappa = 1.8$, and $\delta = 0.0$.

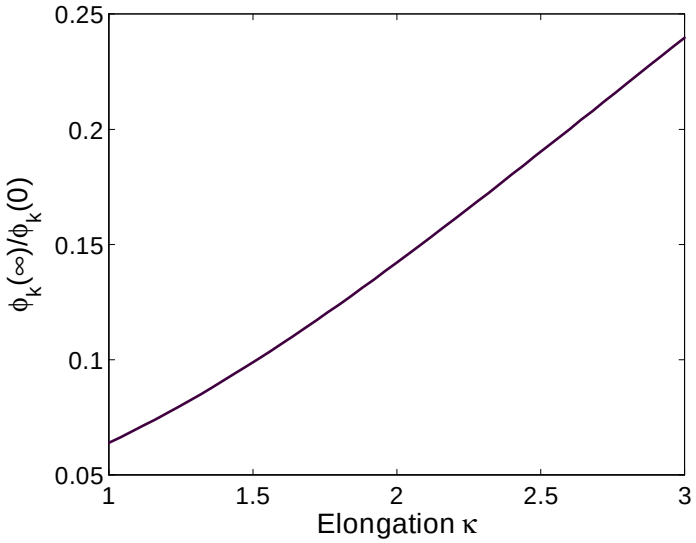

Figure 1

Y. Xiao, P.J. Catto

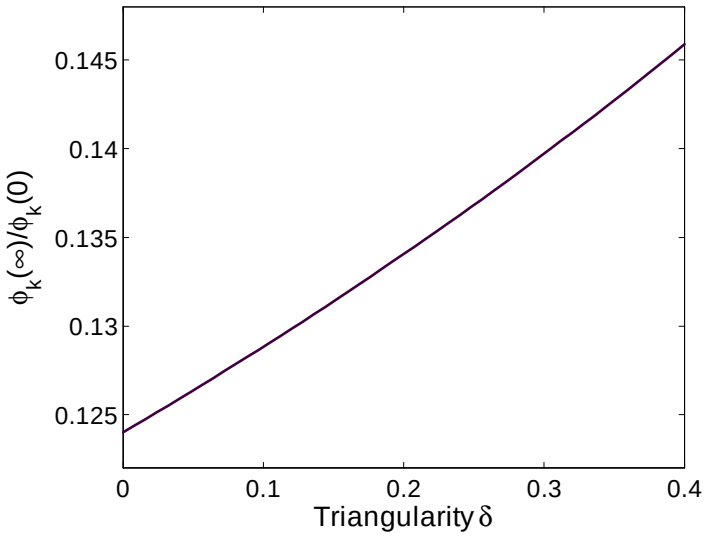

Figure 2

Y. Xiao, P.J. Catto

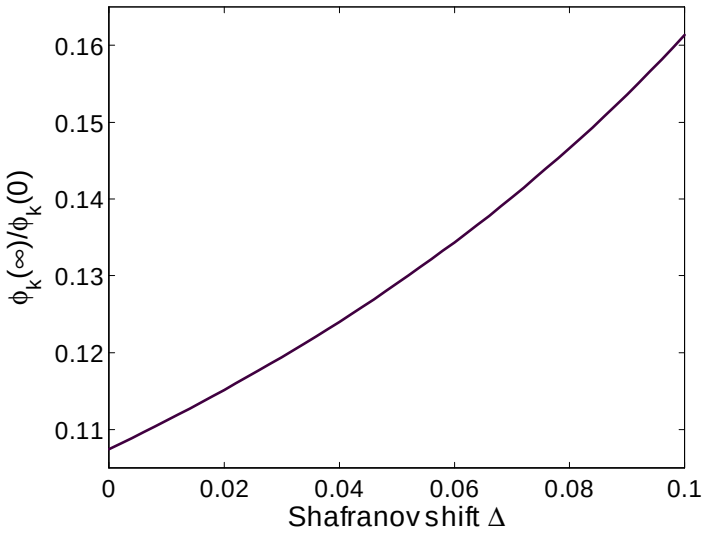

Figure 3

Y. Xiao, P.J. Catto